Recovery of Fe and V via selective reduction–magnetic separation of vanadium-titanium magnetite concentrate

Liwei Liu [1], Guofeng Li [1], Libing Zhao [1], Jinpeng Li [2], Yanfeng Li [1]

[1] College of Mining Engineering, North China University of Science and Technology, Tangshan 063210, China
[2] Mine Design Co., Ltd. of HBIS, Tangshan 063700, China

Corresponding author: liguofengncu@sina.com (G. Li)

Abstract: With the aim of separating Fe and V, a vanadium-titanium magnetite concentrate was selectively reduced, followed by magnetic separation. The processes accompanying reduction of the vanadium-titanium magnetite concentrate were investigated using thermodynamic simulation, experiments, scanning electron microscopy, and electron probe microanalysis. Appropriate reduction conditions and controlling the amount of $CaCO_3$ promoted the reduction of Fe-containing minerals to metallic Fe. V was released from magnetite, ilmenite, and titanomagnetite, and was inhibited to reduce to metallic V, leading to V enrichment in the non-magnetic products in the form of oxides. Moreover, the Fe particles wrapped the slag phase when the amount of $CaCO_3$ exceeded 8%, which is unfavourable for the magnetic separation of Fe and V. Magnetic products with an Fe content of 87.19%, Fe recovery of 82.62%, V content of 0.09% and non-magnetic products with a V content of 1.00% and a V recovery of 85.49% were obtained when the vanadium-titanium magnetite concentrate was reduced for 100 min at 1623 K with a C/O molar ratio of 2.5 and 8% $CaCO_3$, followed by separating at a magnetic field strength of 85 mT.

Keywords: vanadium-titanium magnetite concentrate, selective reduction, magnetic separation, Fe and V separation

1. Introduction

Global vanadium reserves stand at approximately 22 million tons, of which China's contribution is 9.5 million tons. Vanadium-titanium magnetite (VTM) is the main raw material for V products, where approximately 16% of V products are derived from VTM and 68% from V-rich slag produced by smelting VTM.

VTM is mainly processed using the blast furnace method (Fu et al., 2011a; Fu et al., 2011b; Hu et al., 2013). Before smelting, VTM is usually magnetically separated to obtain vanadium-titanium magnetite concentrate (VTMC). The VTMC is then proportionally blended with common iron ores, pre-treated by sintering, and smelted in a blast furnace to obtain V-containing molten iron and Ti-containing slag. Ti-containing slag, containing 22–25% TiO_2, is difficult to use, while the V-containing hot metal can be converted to qualified steel and V-rich slag by a converter (Chen et al., 2015; Li et al., 2018). V can be extracted from V-rich slag by sodium salt roasting-water leaching and calcification roasting-acid leaching (Hao et al., 2018; Xiang et al., 2018). The blast furnace method suffers from complicated procedures and high-energy consumption, along with the use of coke as a reducing agent.

In recent years, non-blast furnace methods have been proposed for processing VTMCs, namely direct reduction–electric furnace and direct reduction-magnetic separation (Zhang et al., 2011; Lv et al., 2013; Chen et al., 2014a; Wu et al., 2016; Wang et al., 2019; Gilligan et al., 2020; Qin et al., 2020). In the reduction process, the reducing reagents are not restricted to coke, and the amount of added agents and the reduction reaction can be controlled more accurately (Chen et al., 2014a; Tang et al., 2016; Li et al., 2018; Zeng et al., 2020). For example, Li et al. (2017) used H_2 and CO to reduce the Hongge VTM pellet, where

88.27% V was enriched in molten iron after melting the reduced pellet. To promote the release of Fe from $FeTi_2O_5$, Chen et al. (2017; 2019) used MgO as an additive, where the main phases of the reduction product were metallic Fe and Mg_2TiO_4.

In the direct reduction–electric furnace, the V-containing mineral is reduced to metallic V which migrates to the Fe phase. The reduced VTMC is then smelted separation into crude Fe and V-rich slag using an electric furnace. Geng et al. (2015; 2017) found that titanomagnetite in VTMC was reduced to $Fe_{2.75}Ti_{0.25}O_4 \rightarrow Fe_2TiO_4 \rightarrow FeTiO_3 \rightarrow Fe_2TiO_5$ at 1473 K. An appropriate amount of Na_2SO_4 could promote the reduction of titanomagnetite and growth of the Fe particles. Wu et al. (2016) smelted reduced VTMC at 1823 K with 0.6% alkalinity and 3.59% carbon, when 92.98% crude Fe and Ti slag were obtained. Wang et al. (2020) reported that the distribution ratio for the partitioning of V between the Fe phase and slag phase increases with an increase in the CaO and MgO contents of the initial slag, as well as with the temperature, when the crude Fe is smelted. When the TiO_2 content of the slag was greater than 30%, it was difficult to separate the Fe and slag.

In the case of direct reduction-magnetic separation, the Fe-containing minerals in VTMC are reduced to metallic Fe and form Fe particles; however, V and Ti exist in the form of oxides. Therefore, V and Ti are enriched in the slag phase when the reduction products are separated by magnetic separation. (Geng et al., 2015; 2017; Qin et al., 2020). Zhao et al. (2015) found that increasing the temperature and amount of reducing agent promoted the reduction of FeV_2O_4 and the enrichment of V in the Fe phase, which is unfavourable for the magnetic separation of Fe and V. Chen et al. (2014b) hot briquetted a mix of VTMC and coal at 748 K, followed by reduction for 60 min at 1623 K. When the reduction products were separated at a magnetic field strength of 50 mT, iron powder and non-magnetic products were obtained, with a V recovery of 61.82% and Ti recovery of 85.31%.

In this study, we focus on controlling the reduction conditions and the amount of $CaCO_3$ added to selectively reduce the Fe-containing minerals and inhibit the reduction of V-containing minerals. The results provide details for the separation of Fe and V from VTMC using selective reduction-magnetic separation technology.

2.   Materials and methods

2.1. Materials

The VTMC used in this study was obtained from the Chengde, Hebei Province, China. The ore sample comprises 61.08% TFe, 7.66% TiO_2, 0.41% V, 2.39% SiO_2, 2.45% Al_2O_3, 0.90% MgO, and 0.14% CaO.

The mineral composition and distribution of the main elements Fe, V, and Ti in VTMC were investigated, and the results are shown in Fig. 1. VTMC is mainly composed of magnetite, ilmenite, titanomagnetite, chlorite, apatite, pyroxene, and corundum as indicated by points 1 to 7, respectively. No independent V-containing minerals were observed because of their low content in the ore sample. Fig. 1(b)–(d) shows that V was associated with Fe and Ti; namely, V is distributed in magnetite, ilmenite, and titanomagnetite in the form of isomorphs.

Coal from Baishan, Jilin province was used as a reducing agent. Proximate analysis of the coal was carried out according to the national standard GB/T 212-2008, and the results showed that the coal was mainly composed of 71.08% fixed carbon, 17.04% volatile matter, 10.78% ash, and 1.10% moisture.

Analytically pure $CaCO_3$ and sodium carboxymethyl starch were used as additives in this test.

2.2. Methods

VTMC, $CaCO_3$, and sodium carboxymethyl starch (0.8% of the total mass of VTMC and $CaCO_3$) were mixed well with 5% water. The mixture was placed into a 12 mm diameter mould. The pellets were pressed at 20 MPa and dried at 378 K in a constant-temperature blast-oven for 4 h. The dried pellets were loaded into a 120 mL graphite crucible, with a C/O molar ratio of 1.0–3.5 (the molar ratio of C in coal to O in iron oxides of ore). The graphite crucible was placed in a KSL-1700X-A2 high-temperature chamber furnace at 1548–1648 K. After 40–140 min of reduction, the crucible was removed and cooled rapidly by circulating room temperature water. After stripping the residual coal around the pellets, the reduction products were obtained. The reduction products were ground to −0.074 mm using a GJ-I test sample preparation grinding crusher machine. A representative 15 g sample of the ground products
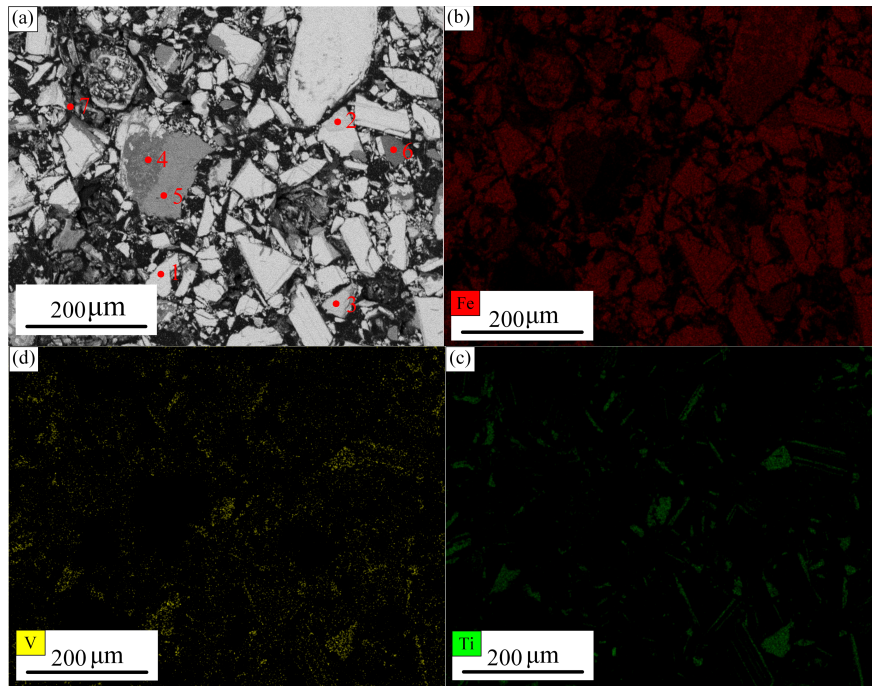
Fig. 1. SEM images of VTMC and distribution of Fe, V, and Ti in VTMC

was separated using an XCSG-Φ50 magnetic separation tube at a magnetic field strength of 85 mT. The magnetic separation tailings were weighed and analysed to determine the V content, and the recovery of V was calculated according to Eq. (1):

$$\varepsilon = \frac{m_t \times \omega_V^t}{m \times \omega_V} \tag{1}$$

where ε (%) is the recovery rate of V, ω_V^t (%) is the V content of the magnetic separation tailings, ω_V (%) is the V content of the reduction products, m (g) is the mass of the representative reduction products, and m_t (g) is the mass of the magnetic separation tailings.
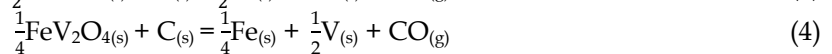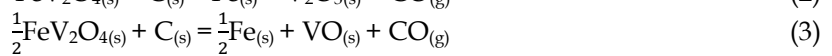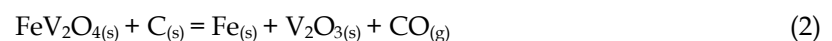
2.3. Analysis and characterization

The chemical composition of the samples was examined by inductively coupled plasma-optical emission spectroscopy (ICP-OES, 6300, Thermo Fisher Scientific, USA). The lifting amount of the test solution was 1.5 mL/min, while the plasma high-frequency emission power was 1350 W.

The microstructure and elemental distribution of VTMC and the reduction products were analysed by scanning electron microscopy integrated with an energy dispersive spectroscope (SEM-EDS, FEI Czech Co., Ltd., Czech Republic). The acceleration voltage was set to 15 kV.

The V content of metallic Fe in the reduction products was investigated using an electron probe microanalyser (EPMA, Japan Electronics Co., Ltd., Japan). The simple Fe and V substances were used as standard samples to calibrate the Fe and V signals.

2.4. Thermodynamic basis for the reduction of V-containing mineral

FeV_2O_4 is usually used for thermodynamic calculation instead of the V-containing mineral in VTMC (Chen et al., 2016; Wang et al., 2020). The following reactions of FeV_2O_4 may occur during the reduction process:

$$FeV_2O_{4(s)} + C_{(s)} = Fe_{(s)} + V_2O_{3(s)} + CO_{(g)} \tag{2}$$

$$\frac{1}{2}FeV_2O_{4(s)} + C_{(s)} = \frac{1}{2}Fe_{(s)} + VO_{(s)} + CO_{(g)} \tag{3}$$

$$\frac{1}{4}FeV_2O_{4(s)} + C_{(s)} = \frac{1}{4}Fe_{(s)} + \frac{1}{2}V_{(s)} + CO_{(g)} \tag{4}$$

$$FeV_2O_{4(s)} + C_{(s)} = FeO_{(s)} + 2VO_{(s)} + CO_{(g)} \tag{5}$$

$$V_2O_{3(s)} + C_{(s)} = 2VO_{(s)} + CO_{(g)} \tag{6}$$

The reduction products of FeV_2O_4 include Fe, FeO, V_2O_3, VO, and V. Metallic V is enriched in the Fe phase and cannot be separated by magnetic separation.

3.   Results and discussion

3.1. Thermodynamic simulations

The equilibrium compositions module of the HSC Chemistry software (6.0) was used to simulate the equilibrium compositions of the final products obtained from the selective reduction-magnetic separation of VTMC. Titanomagnetite ($Fe_{2.75}Ti_{0.25}O_4$) is regarded as a solid solution of magnetite (Fe_3O_4) and ulvospinel (Fe_2TiO_4) (Park and Ostrovski, 2003; Hu et al., 2013; Jung, 2015). It is proposed that the unreacted FeV_2O_4, Fe_2TiO_4, Fe_3O_4 and the newly generated metallic Fe entered the magnetic products and the other oxides entered the non-magnetic products during the magnetic separation process.

3.1.1. Effect of reduction temperature

The Fe_3O_4-$FeTiO_3$-Fe_2TiO_4-FeV_2O_4-Al_2O_3-SiO_2 system, which is closest to the composition of VTMC, was simulated at C/O molar ratios of 1.5–3.0 and with no additives. The effect of the reduction temperature on the selective reduction–magnetic separation of VTMC is shown in Fig. 2.
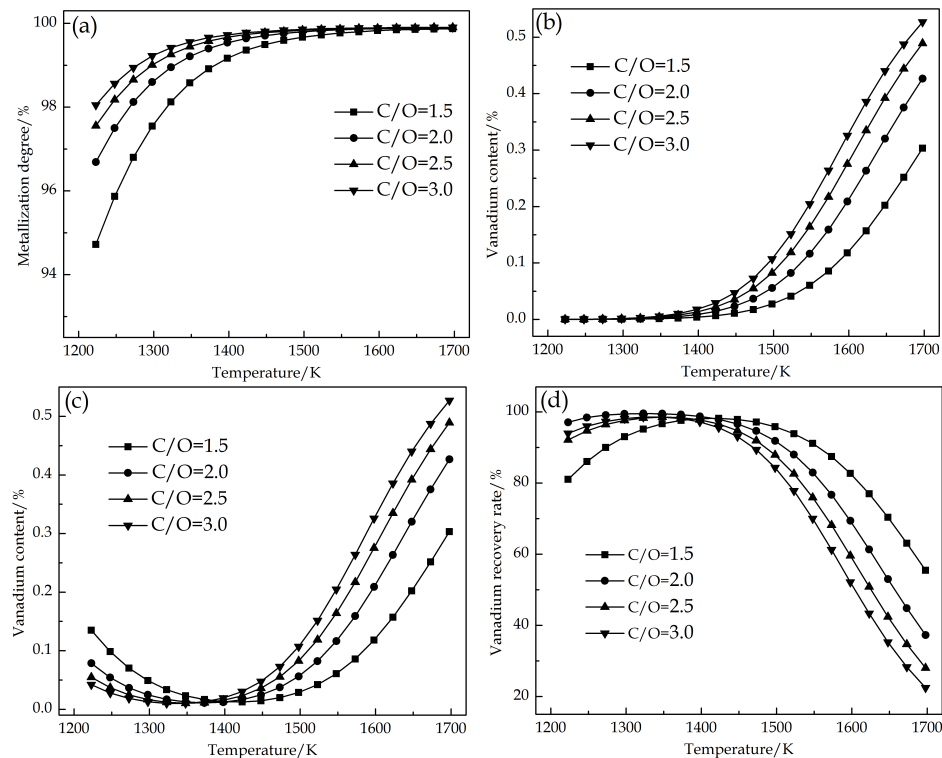

Fig. 2. Effect of reduction temperature on the indexes of products: (a) Fe metallisation rate of reduction products; (b) V content of Fe phase; (c) V content of magnetic products; (d) V recovery of non-magnetic products

As shown in Fig. 2, a higher reduction temperature favours the generation of metallic Fe and V, while the generation of metallic V is initiated when the temperature is increased to 1382 K. The metallic V migrates to the Fe phase, leading to an increase in the concentration of V in the Fe phase with a higher reduction temperature.

At temperatures of <1382 K, FeV_2O_4 was mainly reduced to V oxides. The V oxides migrate to the slag phase and are concentrated in the non-magnetic products. Therefore, the temperature increase resulted in a decrease in the V content in the magnetic products and an increase in the V recovery in the non-magnetic products. At temperatures of >1382 K, metallic V is generated, and the amount increases with increasing temperature. Macroscopically, an increase in temperature results in a higher V content in the magnetic products and lower V recovery in the non-magnetic products.

3.1.2.   Effect of C/O molar ratio on simulation results

The effect of the C/O molar ratio on the metallisation rate of Fe, the V content of the Fe phase, and the magnetic separation performance in the temperature range of 373–1673 K is shown in Fig. 3.
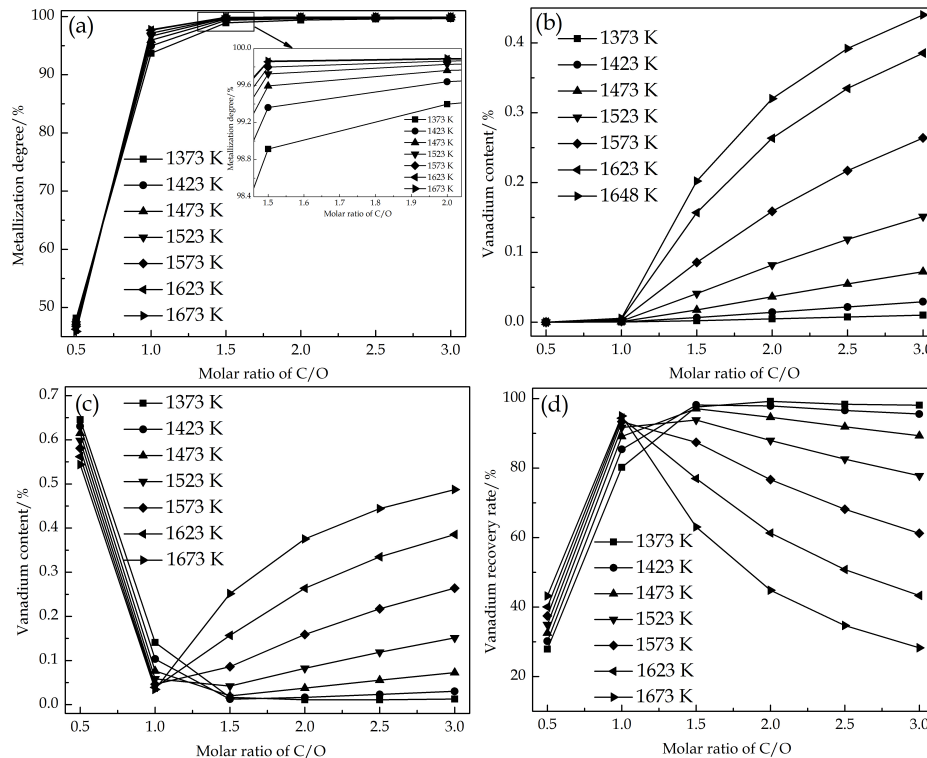

Fig. 3. Effect of C/O molar ratio on the indexes of products: (a) Fe metallisation rate of reduction products; (b) V content of Fe phase; (c) V content of magnetic products; (d) V recovery of non-magnetic products

When the C/O molar ratio was increased from 0.5 to 1.0 (Fig. 3 (a) and (b)), the metallisation rate of Fe increased rapidly, and almost no metallic V was generated. However, when the C/O molar ratio continued to increase, the metallisation of Fe in the reduction products increased slowly and then remained unchanged, and the V content in metallic Fe increased rapidly. This is because the standard Gibbs free energy change for the reduction of FeV_2O_4 to metallic V is higher than that for the reduction of Fe_3O_4, $FeTiO_3$, and Fe_2TiO_4 to metallic Fe (Huang, 2013). Therefore, the Fe-containing minerals were first reduced to metallic Fe when the amount of reducing agent was insufficient. The generation of metallic V occurs when there is a sufficient reducing agent.

As shown in Fig. 3 (c) and (d), for C/O molar ratios of ≤1, increasing the reducing agent resulted in a lower V content in the magnetic products and higher V recovery in the non-magnetic products. When the C/O molar ratio was >1.5, increasing the reducing agent resulted in a higher V content of the magnetic products and lower V recovery in the non-magnetic products. It can be deduced that FeV_2O_4 was mainly reduced to V oxides at C/O molar ratio of ≤1. The V oxides were further reduced to metallic V and migrated to the Fe phase with increasing amounts of reducing agent.

3.1.3. Effect of CaCO₃ on simulation results

The effect of the amount of $CaCO_3$ on the metallisation rate of Fe, the V content of the Fe phase, and the magnetic separation indexes as simulated at a C/O molar ratio of 2.0 (Fig. 4). Fig. 4(a)–(d) shows that increasing the amount of $CaCO_3$ promoted the generation of metallic Fe, and almost no metallic V was formed at ≤1382 K. At a reduction temperature of >1382 K, the amount of metallic V that was generated decreased as the amount of $CaCO_3$ increased. This is shown by the decrease in the V content in the magnetic products and concomitant increase in the V recovery of the non-magnetic products with higher amount of $CaCO_3$. Overall, the addition of an appropriate amounts of $CaCO_3$ can promote the

production of metallic Fe and inhibit the production of metallic V, which is beneficial for the magnetic separation of Fe and V in the reduction products.
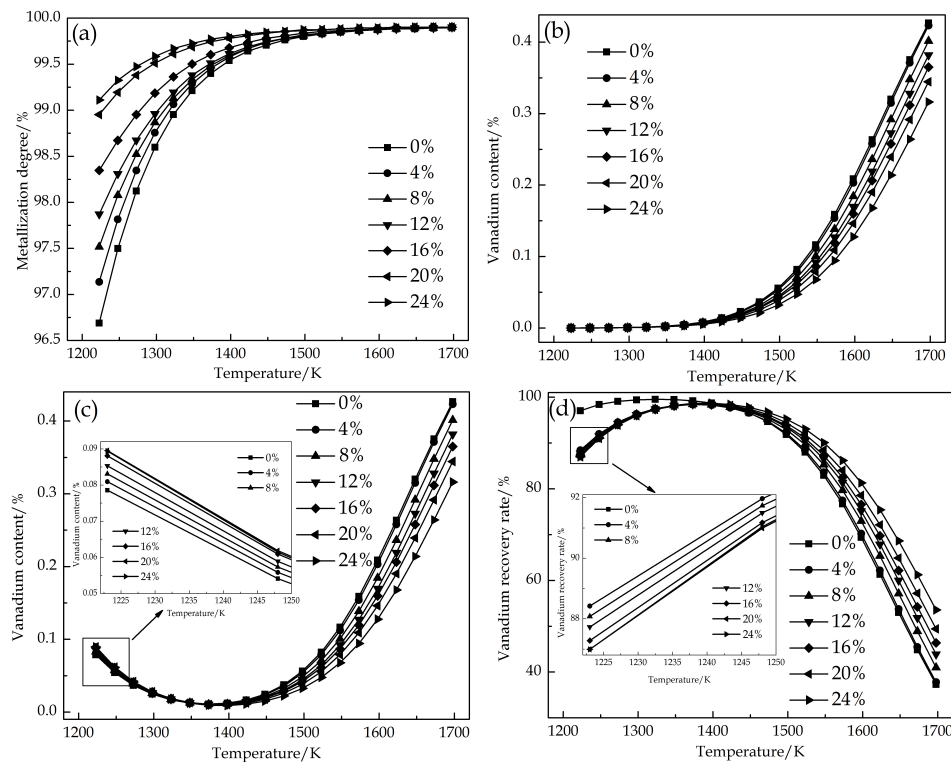

Fig. 4. Effect of $CaCO_3$ addition on the indexes of products: (a) Fe metallisation rate of reduction products; (b) V content of Fe phase; (c) V content of magnetic products; (d) V recovery of non-magnetic products

3.2. Selective reduction of VTMC and magnetic separation of reduction products

3.2.1. Effect of temperature

From the thermodynamic simulation results, VTMC was reduced within 120 min at 1548–1648 K with a 2.5 C/O molar ratio and 16% $CaCO_3$. The results are shown in Fig. 5.

As shown in Fig. 5, a higher temperature increased the metallisation rate of Fe in the reduction products and the Fe content and Fe recovery of the magnetic products. At temperatures of <1623 K, a higher reduction temperature decreased the V content in the magnetic products but increased the V content and V recovery in the non-magnetic products. At temperatures of >1623 K, a higher reduction temperature decreased the V recovery in the non-magnetic products.

This is because the reduction reactions of Fe-containing minerals and V-containing minerals are heat absorption reactions, and the initial temperature of the reduction reaction of Fe-containing minerals is lower than that of V-containing minerals. An increase in temperature favours the reduction of Fe-containing minerals and the release of V oxides from magnetite, ilmenite, and titanomagnetite, which promotes the enrichment of V in the non-magnetic products. However, an increasing number of V oxides is reduced to metallic V and migrated into the metallic Fe phase at temperature above 1623 K. Therefore, the optimal reduction temperature is 1623 K. Under those conditions, magnetic products with an Fe content of 85.02%, Fe recovery of 91.98%, V content of 0.17%, and non-magnetic products with a V content of 0.99% and V recovery of 70.77% were produced.

3.2.2. Effect of reduction time

The effect of the reduction time on the selective reduction–magnetic separation of VTMC was evaluated at a reduction temperature of 1623 K using 16% $CaCO_3$, and a C/O molar ratio of 2.5. The results are shown in Fig. 6.
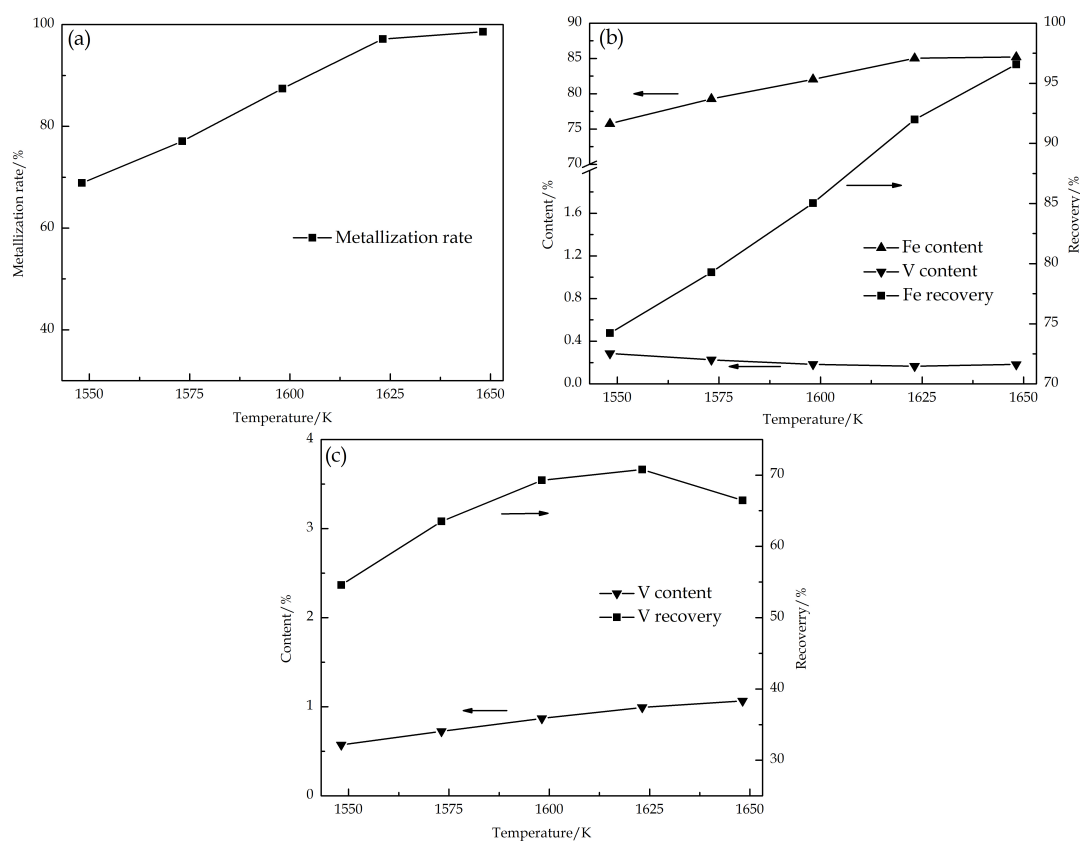
Fig. 5. Effect of temperature on the metallisation rate of reduction products and separation indexes: (a) Fe metallisation rate; (b) indexes of magnetic products; (c) indexes of non-magnetic products
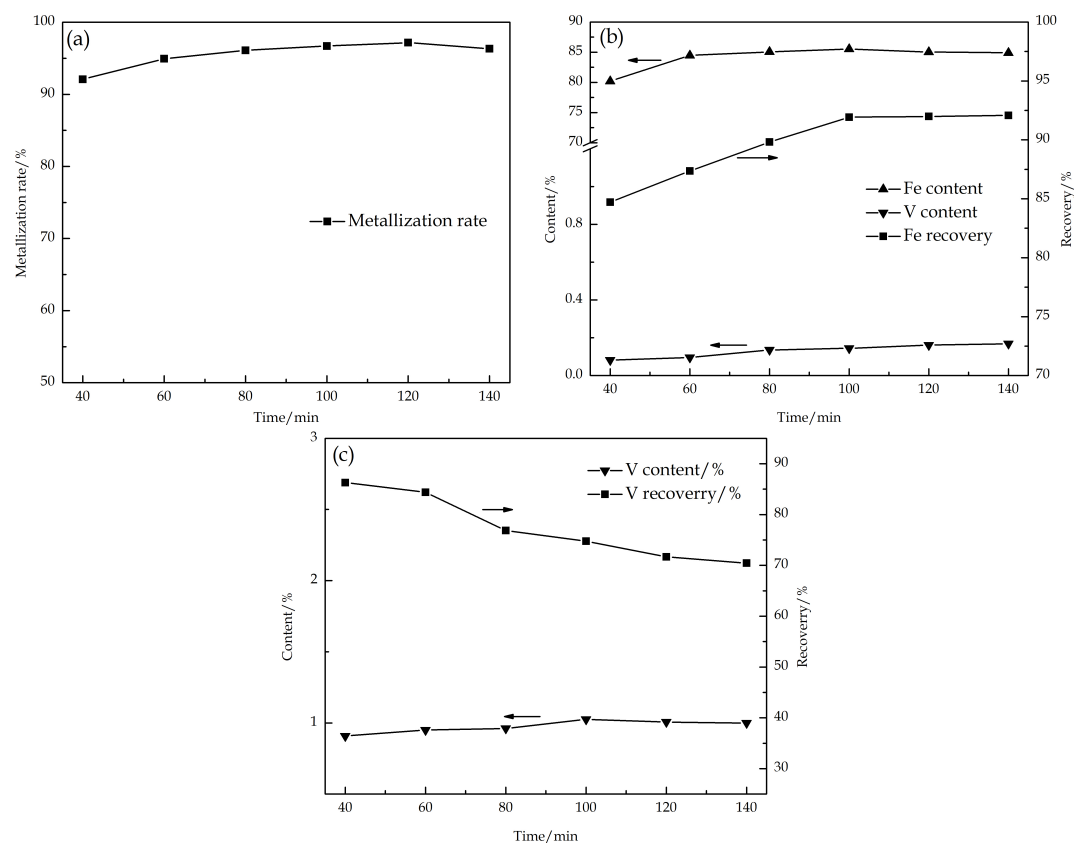

Fig. 6. Effect of reduction time on the metallisation rate of reduction products and separation indexes: (a) Fe metallisation rate; (b) indexes of magnetic products; (c) indexes of non-magnetic products

As shown in Fig. 6, the metallisation rate of Fe, the Fe content, and Fe recovery in the magnetic products increased when the reduction time was increased to 100 min, and then remained almost constant, while the V content increased with time. For the non-magnetic products, increasing the reduction time decreased the V recovery and increased the V content.

This is attributed to the fact that an increasing number of Fe oxides and V oxides is reduced to metallic Fe and V with extending reduction time. Given that the reduction of Fe oxides is easier than that of V oxides, the Fe oxides were almost fully reduced to Fe after 100 min, whereas the reduction of V oxides was not complete within the testing time. Magnetic products with Fe contents of 85.51%, Fe recoveries of 91.92%, and V contents of 0.14% were obtained at a reduction time of 100 min. The non-magnetic products had a V content of 1.03% and V recovery of 74.77%.

3.2.3. Effect of C/O molar ratio

The effect of the C/O molar ratio on the selective reduction–magnetic separation of VTMC was investigated at a reduction temperature of 1623 K, reduction time of 100 min, and $CaCO_3$ content of 16%. The experimental results are shown in Fig. 7.
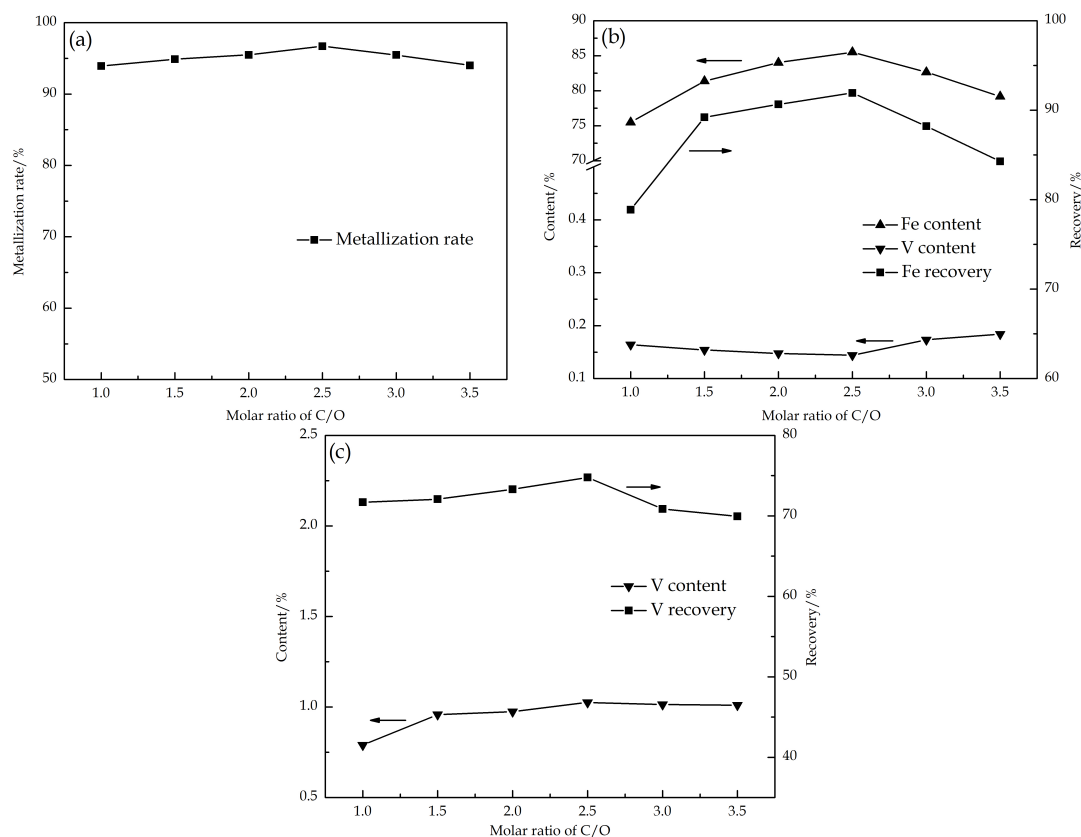

Fig. 7. Effect of the C/O molar ratio on the metallisation rate of reduction products and separation indexes: (a) Fe metallisation rate; (b) indexes of magnetic products; (c) indexes of non-magnetic products

As shown in Fig. 7, when the C/O molar ratio was lower than 2.5, the metallisation rate of Fe and the Fe content and Fe recovery in the magnetic products increased, but the V content decreased with an increase in the C/O molar ratio. The V content and V recovery in the non-magnetic products increased with an increase in the C/O molar ratio. At C/O molar ratios of >2.5, increasing the C/O molar ratio results in a lower Fe content and Fe recovery and a higher V grade in the magnetic products. The V recovery in the non-magnetic products decreased rapidly, and V content was almost unchanged.

This is because the thickness of the coal powder covering the VTMC pellets increases with an increase in the amount of coal, which is not conducive to the diffusion of CO from the environment to the surface of the pellets and hinders the reduction reaction. V oxides inside the lattice of magnetite, ilmenite, and titanomagnetite increased the V content in the magnetic products. The Fe content in the

magnetic products decreased concomitantly because the Fe content of magnetite and titanomagnetite is lower than that of metallic Fe. When the C/O molar ratio was 2.5, the magnetic products contained 85.51% Fe and 0.14% V, with an Fe recovery of 91.92%. The V content and V recovery in the non-magnetic products were 1.03% and 74.77%, respectively.

3.2.4. Effect of CaCO₃ amount

Fig. 8 shows the effect of the amount of $CaCO_3$ on the selective reduction–magnetic separation of VTMC at a reduction temperature of 1623 K, reduction time of 100 min, and C/O molar ratio of 2.5.
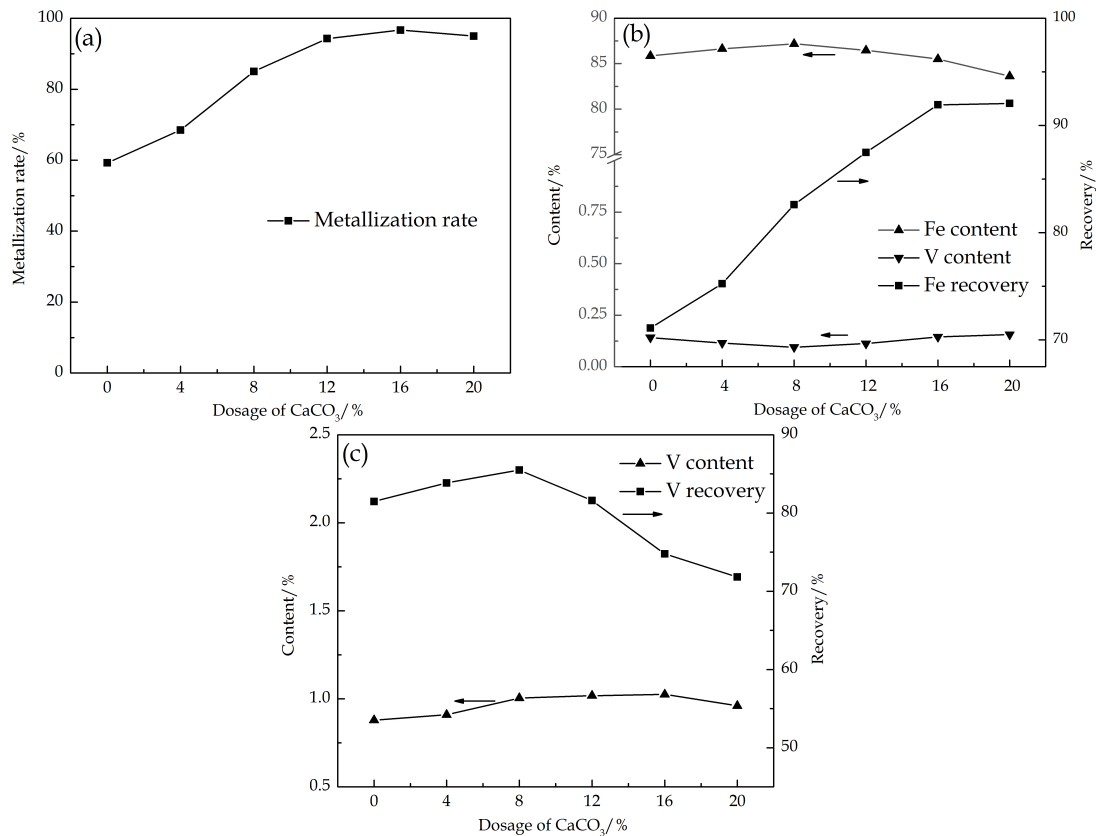

Fig. 8. Effect of $CaCO_3$ amount on the metallisation rate of reduction products and separation indexes: (a) Fe metallisation rate; (b) indexes of magnetic products; (c) indexes of non-magnetic products

As shown in Fig. 8, when the amount of $CaCO_3$ was <16%, the metallisation rate of Fe and the Fe recovery in the magnetic products increased as the amount of $CaCO_3$ increased, showing that the appropriate concentration of $CaCO_3$ can promote the generation of metallic Fe. When the amount of $CaCO_3$ was <8%, the Fe content of the magnetic products and the V content and V recovery in the non-magnetic products increased with increasing $CaCO_3$ content. With >8% $CaCO_3$, the Fe content of the magnetic products and V recovery in the non-magnetic products decreased with an increase in the $CaCO_3$ amount.

The V content in the magnetic products and V recovery in the non-magnetic products did not match the simulation results. This may be because the growing Fe particles wrapped the slag phase, preventing complete dissociation during the grinding process. Concomitantly, the V content in the magnetic products increased and the V recovery in the non-magnetic products decreased. With 8% $CaCO_3$, the magnetic products had a Fe content of 87.19%, Fe recovery of 82.62%, and V content of 0.09%. The V content and V recovery for the corresponding non-magnetic products were 1.00% and 85.49%, respectively.

Overall, the Fe recovery in the magnetic products and the V recovery in the non-magnetic products obtained from the tests were lower than those of the simulation results. This is attributed to the fact that the thermodynamic simulations target the ideal reaction system, regardless of the effect of the reduction

rate. Moreover, complete (100%) liberation and magnetic separation of the magnetic from the non-magnetic products were not achieved in the tests.

3.3. Effect of CaCO₃ on phase composition of reduction products and morphology of Fe particles

3.3.1. Effect of CaCO₃ on phase composition of reduction products

The effect of $CaCO_3$ on the phase composition of the reduction products at 1623 K after 100 min reduction time, with 2.5 C/O molar ratio is shown in Fig. 9. As shown there, peaks of metallic Fe, wustite ($Fe_{1-x}O$), titanomagnetite ($Fe_{2.75}Ti_{0.25}O_4$), Ti–Fe spinel ($Fe_{2.5}Ti_{0.5}O_4$), and fayalite (Fe_2SiO_4) were observed in the XRD pattern of the reduction products in the absence of $CaCO_3$. As the amount of $CaCO_3$ increased, the peaks of metallic Fe intensified, whereas those of titanomagnetite, fayalite, and Ti–Fe spinel became smaller. The peaks of titanomagnetite and fayalite disappeared at a $CaCO_3$ content of 4%, while the peaks of Ti–Fe spinel disappeared when the $CaCO_3$ content increased to 8%. The intensity of the wustite peak increased as the amount of $CaCO_3$ increased to 8% but decreased with a further increase in the amount of $CaCO_3$.

Peaks of perovskite ($CaTiO_3$) were observed when the $CaCO_3$ amount reached 8%, and became larger with a further increase in the amount of $CaCO_3$. Peaks of Mg-Al spinel ($Mg_2(Al,Fe)_2O_4$) and gehlenite ($Ca_2Al(Al, Si)O_7$) were observed with $CaCO_3$ contents above 12% and 16%, respectively. The peaks of Mg-Al spinel became less intense, whereas the peaks of gehlenite intensified with increasing $CaCO_3$ content. No independent V-containing mineral was detected as this was present in low content.
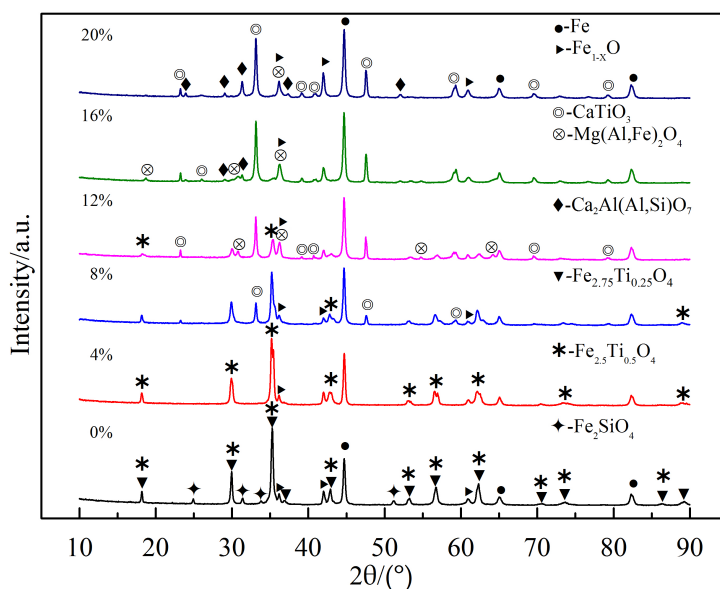

Fig. 9. XRD patterns of the reduction products obtained with different amounts of CaCO₃

3.3.2. Effect of CaCO₃ on morphology of Fe particles

SEM images showing the morphology of the Fe particles obtained with different amounts of $CaCO_3$ are presented in Fig. 10. As shown in Fig. 10, the Fe particles did not wrap the slag when the added $CaCO_3$ was <8%. Slag inside the Fe particles was observed with 12% $CaCO_3$. Moreover, the slag phase was more extensively wrapped by the Fe particles as the amount of $CaCO_3$ further increased, which is not conducive to the liberation of Fe particles and slag during the grinding process. The separation of Fe particles and slag became more difficult. Therefore, the addition of $CaCO_3$ should be controlled within 8%.

To accurately determine the V content of the Fe phase, the V content in metallic Fe with the use of various amounts of $CaCO_3$ was analysed using EPMA. The results are shown in Table 1. The V content in the Fe phase decreased as the amount of $CaCO_3$ increased (Table 1), indicating that $CaCO_3$ inhibited the production of metallic V and facilitated the magnetic separation of Fe and V in the reduction products, which is consistent with the results of the simulation and experiment.
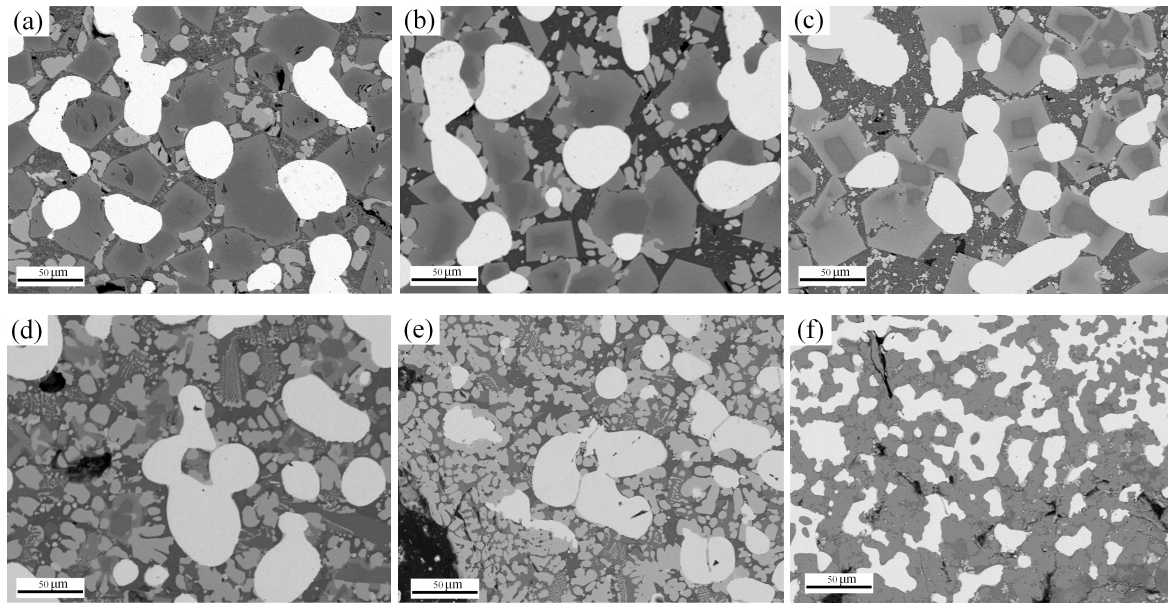
Fig. 10. SEM images of the reduction products obtained with different amounts of CaCO$_3$: (a) 0%; (b) 4%; (c) 8%; (d) 12%; (e) 16%; (f) 20%

Table 1 V content of Fe phase with different amounts of CaCO$_3$ (wt. %)

Amount	Position				Average
	1	2	3	4	
0%	0.153	0.126	0.098	0.165	0.136
4%	0.149	0.094	0.126	0.104	0.118
8%	0.071	0.107	0.085	0.113	0.094
12%	0.071	0.126	0.051	0.094	0.086
16%	0.019	0.142	0	0.112	0.068
20%	0.013	0	0.082	0	0.024

4. Conclusion

Based on thermodynamic simulations, selective reduction-magnetic separation of VTMC was conducted. The phase compositions of the reduction products and morphology of the Fe particles were analysed. The following conclusions were derived based on the results.

(1) The simulation results indicate that increasing the reduction temperature and C/O molar ratio promoted the reduction of Fe-containing and V-containing minerals. Metallic V is more difficult to generate than Fe, which can be generated at temperatures above 1382 K and C/O molar ratios above 1.0. An excessive temperature or C/O molar ratio is unfavourable for the enrichment of V in the slag phase. An appropriate amount of CaCO$_3$ promotes the generation of metallic Fe and inhibits the generation of metallic V, which is beneficial for the separation of Fe and V.

(2) The suitable conditions for reducing VTMC were determined to be 1623 K temperature, 100 min reduction time, 2.5 C/O molar ratio, and 8% added CaCO$_3$. Magnetic products with an Fe content of 87.19%, Fe recovery of 82.62%, and V content of 0.09% were produced by selective reduction followed by magnetic separation. Moreover, non-magnetic products with a V content of 1.00% and V recovery of 85.49% were obtained.

(3) The addition of CaCO$_3$ affects the phase composition of the reduction products and the morphology of the Fe particles. Compared with no CaCO$_3$, the addition of 8% CaCO$_3$ can decrease the wustite, titanomagnetite, and Ti–Fe spinel content in the reduction products and increase the content of metallic Fe. Moreover, adding >8% CaCO$_3$ results in the Fe particles wrapping the slag phase, which is unfavourable for the separation of Fe and V.

Acknowledgments

References

CHEN, S. Y., CHU, M. S., 2014a. *A new process for the recovery of iron, vanadium, and titanium from vanadium titanomagnetite*. J. South. Afr. Inst. Min. Metall. 114, 481-487.

CHEN, S. Y., CHU, M. S., 2014b. *Metalizing reduction and magnetic separation of vanadium titano-magnetite based on hot briquetting*. Int. J. Miner., Metall. Mater. 21, 225-233.

CHEN, S. Y., FU, X., CHU, M. S., 2015. *Life cycle assessment of the comprehensive utilisation of vanadium titano-magnetite*. J. Cleaner Prod. 101, 122-128.

CHEN, S. Y., FU, X., CHU, M. S., 2016. *Carbothermic Reduction Mechanism of Vanadium-titanium Magnetite*. J. Iron Steel Res. Int. 23, 409-414.

CHEN, C., SUN, T. C., WANG, X. P., 2017. *Effects of MgO on the Reduction of Vanadium Titanomagnetite Concentrates with Char*. JOM. 69, 1759-1766.

CHEN, C., SUN. T., KOU, J., WANG, X., ZHAO, Y., 2019. *Feasibility study on preparation of magnesium titanate in carbonthermic reduction of vanadium titanomagnetite concentrates*. Physicochem. Probl. Miner. Process., 55, 417-425.

FU, W., WEN, Y, XIE, H., 2011a. *Development of Intensified Technologies of Vanadium-Bearing Titanomagnetite Smelting*. J. Iron Steel Res. Int. 18, 7-18.

FU, W., XIE, H., 2011b. *Progress in Technologies of Vanadium-Bearing Titanomagnetite Smelting in PanGang*. Steel Res. Int. 82, 501-504.

GENG, C., SUN, T. C., YANG, H., 2015. *Effect of Na$_2$SO$_4$ on the Embedding Direct Reduction of Beach Titanomagnetite and the Separation of Titanium and Iron by Magnetic Separation*. ISIJ Int. 55, 2543-2549.

GENG, C., SUN, T. C., MA, Y., 2017. *Effects of embedding direct reduction followed by magnetic separation on recovering titanium and iron of beach titanomagnetite concentrate*. J. Iron Steel Res. Int. 24, 156-164.

GILLIGAN, R., NIKOLOSKI, A. N., 2020. *The extraction of vanadium from titanomagnetites and other sources*. Miner. Eng. 146.

HU, T., LV, X., BAI, C., LUN, Z., 2013. *Reduction Behavior of Panzhihua Titanomagnetite Concentrates with Coal*. Metall. Mater. Trans. B. 44, 252-260.

HUANG, X., 2013. I*ron and steel metallurgy principle*. Metallurgical Industry Press. Beijing, China.

HAO, P., GUO, J., ZHENG X., LIU, Z., TAO, C., 2018. *Leaching Kinetics of Vanadium from Calcification Roasting Converter Vanadium Slag in Acidic Medium*. J. Environ. Chem. Eng., 6, 5119-5124.

JUNG, S. M., 2015. *Effects of CaO/CaCO$_3$ on the Carbothermic Reduction of Titanomagnetite Ores*[J]. Metall. Mater. Trans. B. 46, 1162–1174.

LV, X., LUN, Z., YIN, J., 2013. *Carbothermic Reduction of Vanadium Titanomagnetite by Microwave Irradiation and Smelting Behavior*. ISIJ Int., 53, 1115-1119.

LI, W., FU, G. Q., CHU, M. S., 2017. *Reduction behavior and mechanism of Hongge vanadium titanomagnetite pellets by gas mixture of H$_2$ and CO*. J. Iron Steel Res. Int. 24, 34-42.

LI, W., FU, G., CHU, M., ZHU, M., 2018. *Influence of V$_2$O$_5$ content on the gas-based direct reduction of hongge vanadium titanomagnetite pellets with simulated shaft furnace gases*. JOM, 70, 76−80.

PARK, E., OSTROVSKI, O., 2003. Reduction of Titania-Ferrous Ore by Carbon Monoxide. ISIJ Int. 43, 1316-1325.

QIN, J., WANG, Y., YOU, Z., 2020. *Carbonization and nitridation of vanadium–bearing titanomagnetite during carbothermal reduction with coal*. J. Mater. Res. Technol. 9, 4272-4282.

TANG, J., CHU, M., FENG, C., 2016. *Melting Separation Behavior and Mechanism of High-chromium Vanadium–bearing Titanomagnetite Metallized Pellet Got from Gas-based Direct Reduction*. ISIJ Int. 56, 210-219.

WANG, S., GUO, Y., JIANG, T., 2019. *Behavior of Silicon During Reduction and Smelting of Vanadium Titanomagnetite Metallized Pellets in an Electric Furnace*. JOM. 71, 329-335.

WANG, S., GUO, Y. F., ZHENG, F. Q., 2020. *Behavior of vanadium during reduction and smelting of vanadium titanomagnetite metallized pellets*. Trans. Nonferrous Met. Soc. China. 30, 1687-1696.

WU, E. H., ZHU, R., YANG, S. L., 2016. *Influences of Technological Parameters on Smelting-separation Process for Metallized Pellets of Vanadium-bearing Titanomagnetite Concentrates*. J. Iron Steel Res. Int. 23, 655-660.

XIANG, J. Y., HUANG, Q., LV, X., BAI, C., 2018. *Extraction of vanadium from converter slag by two-step sulfuric acid leaching process*. J. Cleaner Prod., 170, 1089-1101.

ZHANG, W., ZHU, Z., CHENG, C. Y., 2011. *A literature review of titanium metallurgical processes*. Hydrometallurgy. 108, 177-188.

ZHAO, L., WANG, L., CHEN, D., ZHAO, H., 2015. B*ehaviors of vanadium and chromium in coal-based direct reduction of high-chromium vanadium-bearing titanomagnetite concentrates followed by magnetic separation. Trans.* Nonferrous Met. Soc. China, 25, 1325-1333.

ZENG, R., LI, W., WANG, N., 2020. *Effect of Al₂O₃ on the gas-based direct reduction behavior of Hongge vanadium titanomagnetite pellet under simulated shaft furnace atmosphere*. Powder Technol. 376, 342-350.